MEDWIN PUBLISHERS
Committed to create value for Researchers

Food Science and Nutrition Technology
ISSN: 2574-2701

# Evaluation of the Consciousness Energy Healing Treated Berberine Chloride Using PXRD, PSA, and DSC Analysis

**Nayak G[1], Trivedi MK[1], Branton A[1], Trivedi D[1] and Jana S[2]***

[1]Trivedi Global, Inc., Henderson, USA

[2]Trivedi Science Research Laboratory Pvt. Ltd., Bhopal, India

***Corresponding author:** Snehasis Jana, Trivedi Science Research Laboratory Pvt. Ltd., Bhopal, India, Tel: +91-022-25811234; Email: publication@trivedieffect.com

**Research Article**

Volume 3 Issue 6

**Received Date**: November 01, 2018

**Published Date:** December 15, 2018

**DOI:** 10.23880/fsnt-16000168

## Abstract

Berberine is one of the well-known traditional Chinese medicines and it has been significantly effective against various ailments. This study was performed to evaluate the effect of the Trivedi Effect®-Consciousness Energy Healing Treatment on its physicochemical properties by using PXRD, PSA, TGA/DTG, and DSC analytical techniques. The sample was divided into two parts; the first part was considered as a control sample (without treatment), while the second part was received the Consciousness Energy Healing Treatment remotely by the Biofield Energy Healer, Gopal Nayak and denoted as the treated sample. The PXRD peak intensities and crystallite sizes were altered ranging from -28.78% to 115.15% and -15.76% to 241.38%, respectively; however the average crystallite size was increased significantly by 23.05% in the treated sample compared to the control sample. The particle sizes were significantly increased by 16.89% ($d_{10}$), 34.41% ($d_{50}$), 21.88% ($d_{90}$), and 22.85 % {D (4,3)}, which resulted in the significant increase in the specific surface area by 14.74% in the treated sample compared to the control sample. The thermal analysis indicated 3.98% increase in weight loss and 3.64% decrease in the residue weight of the treated sample compared to the control sample. The latent heat for the 1st, 2nd, 3rd, 4th, 5th, and 6th peaks of the treated sample were significantly altered by 224.78%, 7.93%, 8.92%, -9.05%, -45.82%, and 10.93%, respectively, compared to the control sample. The overall analysis indicated that the Trivedi Effect®-Consciousness Energy Healing Treated berberine chloride might possess better solubility, absorption, and thermal stability compared to the untreated sample. Thus, the Trivedi Effect® could be used in improving the bioavailability of berberine chloride and might be used for designing the novel nutraceutical/pharmaceutical formulations to combat various diseases.

**Keywords:** Berberine Chloride; Consciousness Energy Healing Treatment; The Trivedi Effect®; Complementary and Alternative Medicine; Particle Size; PXRD; TGA/DTG

## Introduction

Berberine is very popular and one of the well-known traditional Chinese medicines. It is significantly effective against various ailments [1]. It is an isoquinoline alkaloid with a wide variety of pharmacological importance and is reported to be found in the handful of plants widely used in botanical medical practice such as Golden seal (Hydrastis canadensis), Oregon grape (Berberis aquifolium), Barberry (Berberis vulgaris), and Chinese Goldthread (Coptis chinensis) [2]. The other important medicinal plants reported containing berberine are Phellodendron chinense and Phellodendron amurense [3]. The mechanism of action of berberine underlying on human health is through the action of the adenosine monophosphate-activated protein kinase (AMPK) [4,5]. Further, it was found that AMPK work by regulating an array of biological activities, through which the lipid, glucose, and energy imbalances can significantly normalize [6]. Among various natural supplements for maintaining the overall health, berberine is one of the effective and useful available sources that affect the body at a molecular level. The berberine products such as gel-based berberine can significantly reduce the pain, redness, oozing, and the ulcer size in people with canker sores [7]. In addition, it can be significantly used to control various pathological conditions such as polycystic ovary syndrome, congestive heart failure, liver diseases, hepatitis, gastric ulcers, diabetes, high cholesterol, high blood pressure, burns, diarrhea, glaucoma, menopausal symptoms, metabolic syndromes, obesity, osteoporosis, thrombocytopenia, trachoma, etc [8-12]. However, it was studied that berberine was poorly absorbed across the gut wall and mostly metabolized in the liver through phase I demethylation and phase II glucuronidation, after which the metabolites are excreted with the bile [13,14]. Therefore, researchers are making their effort to enhance the bioavailability of bereberine and mainly focus on its physicochemical properties [15].

In this regard, the Biofield Energy Healing Treatment is one of the best studied Complementary and Alternative Medicine (CAM) that was performed and accepted worldwide. Different kinds of Energy Healing Therapies have been reported with significant clinical and non-clinical outcomes [16,17]. However, the Energy Healing Therapies have been accepted by the U.S. population and is well characterized by the National Center for Complementary and Alternative Medicine (NCCAM) [18,19]. The CAM therapies including Johrei, Reiki, therapeutic touch, yoga, Qi Gong, polarity therapy, Tai Chi, pranic healing, deep breathing, chiropractic/osteopathic manipulation, guided imagery, meditation, massage, homeopathy, hypnotherapy, progressive relaxation, acupressure, acupuncture, special diets, relaxation techniques, Rolfing structural integration, healing touch, movement therapy, pilates, mindfulness, Ayurvedic medicine, traditional Chinese herbs and medicines in biological systems. The Trivedi Effect®-Consciousness Energy Healing therapies have been widely accepted worldwide. Consciousness Energy Healing Treatment found to be significant to improve the physicochemical properties of metals [20-22], improved crop yield [23,24] microbiology [25-27], biotechnology [28,29], improved bioavailability of many compounds [30-32], improved skin health [33,34], improved properties of nutraceuticals [35,36] cancer science research [37,38] and improved overall bone health [39-41]. This study was done to evaluate the effect of Biofield Energy Treatment on the physicochemical and thermal properties of berberine chloride in comparison to the untreated one, by using various analytical techniques.

## Materials and Methods

### Chemicals and Reagents

Berberine chloride was purchased from Tokyo Chemical Industry Co., Ltd., Japan. All other chemicals used during the experiments were of analytical grade available in India.

### Consciousness Energy Healing Treatment Strategies

The berberine chloride sample considered for the experiment was divided into two equal parts. One part of berberine chloride sample was considered as a control sample where no Biofield Energy Treatment was provided. However, the second part of berberine chloride was received the Trivedi Effect®-Consciousness Energy Healing Treatment remotely under standard laboratory conditions for 3 minutes and known as the Biofield Energy Treated berberine chloride sample. This Biofield Energy Treatment was provided through the healer's unique energy transmission process by the renowned Biofield Energy Healer, Gopal Nayak, USA, to the test sample. Further, the control sample was treated with a "sham" healer for comparison purpose. The "sham" healer did not have any knowledge about the Trivedi Effect®-Consciousness Energy Healing Treatment. After that, the Biofield Energy Treated and untreated samples were kept in sealed conditions and characterized using PXRD, PSA, TGA/DTG, and DSC techniques.

### Characterization

**Powder X-ray Diffraction (PXRD) Analysis:** The PXRD analysis of the control and Biofield Energy Treated

berberine chloride was performed with the help of Rigaku Mini Flex-II Desktop X-ray diffractometer (Japan) [42,43]. The Cu Kα radiation source tube output voltage used was 30 kV and tube output current was 15 mA. Scans were performed at room temperature. The average size of individual crystallites were calculated from XRD data using the Scherrer's formula 1:

$$G = k\lambda/\beta\cos\theta \quad (1)$$

Where k is the equipment constant (0.94), G is the crystallite size in nm, λ is the radiation wavelength (0.154056 nm for Kα1 emission), β is the full-width at half maximum (FWHM), and θ is the Bragg angle [44].

The % change in crystallite size (G) of Berberine chloride was calculated using the following equation 2:

$$\%\ \text{change in crystallite size} = \frac{[G_{\text{Treated}} - G_{\text{Control}}]}{G_{\text{Control}}} \times 100 \quad (2)$$

Where $G_{Control}$ and $G_{Treated}$ are the crystallite size of the control and Biofield Energy Treated samples, respectively.

**Particle Size Analysis (PSA):** The particle size analysis of berberine chloride samples were conducted on Malvern Mastersizer 2000, from the UK with a detection range between 0.01 µm to 3000 µm using wet method [45]. The percent change in particle size (d) for at below 10% level ($d_{10}$), 50% level ($d_{50}$), 90% level ($d_{90}$),and D(4,3) was calculated using the following equation 3:

$$\%\ \text{change in particle size} = \frac{[d_{\text{Treated}} - d_{\text{Control}}]}{d_{\text{Control}}} \times 100 \quad (3)$$

Where $d_{Control}$ and $d_{Treated}$ are the particle size (µm) for at below 10% level ($d_{10}$), 50% level ($d_{50}$), and 90% level ($d_{90}$) of the control and Biofield Energy Treated berberine chloride samples, respectively.

The % change in surface area (S) was calculated using the following equation 4:

$$\%\ \text{change in surface area} = \frac{[S_{\text{Treated}} - S_{\text{Control}}]}{S_{\text{Control}}} \times 100 \quad (4)$$

Where $S_{Control}$ and $S_{Treated}$ are the surface area of the control and Biofield Energy Treated berberine chloride samples, respectively.

**Thermal Gravimetric Analysis (TGA)/ Differential Thermogravimetric Analysis (DTG):** TGA/DTG thermograms of the control and Biofield Energy Treated berberine chloride were obtained with the help of TGA Q50TA instruments. A sample of 4-15 mg was loaded to the platinum crucible at a heating rate of 10°C/min from 25°C to 1000°C with the recent literature [46]. The % change in weight loss (W) was calculated using the following equation 5:

$$\%\ \text{change in weight loss} = \frac{[W_{\text{Treated}} - W_{\text{Control}}]}{W_{\text{Control}}} \times 100 \quad (5)$$

Where $W_{Control}$ and $W_{Treated}$ are the weight loss of the control and Biofield Energy Treated berberine chloride, respectively.

The % change in maximum thermal degradation temperature ($T_{max}$) (M) was calculated using the following equation 6:

$$\%\ \text{change in Tmax (M)} = \frac{[M_{\text{Treated}} - M_{\text{Control}}]}{M_{\text{Control}}} \times 100 \quad (6)$$

Where $M_{Control}$ and $M_{Treated}$ are the $T_{max}$ values of the control and Biofield Energy Treated berberine chloride, respectively.

**Differential Scanning Calorimetry (DSC):** The DSC analysis of berberine chloride was performed with the help of DSC Q200, TA instruments. A sample of ~1-5 mg was loaded to the aluminium sample pan at a heating rate of 10°C/min from 30°C to 350°C [46]. The % change in melting point (T) was calculated using the following equation 7:

$$\%\ \text{change in melting point} = \frac{[T_{\text{Treated}} - T_{\text{Control}}]}{T_{\text{Control}}} \times 100 \quad (7)$$

Where $T_{Control}$ and $T_{Treated}$ are the melting point of the control and treated samples, respectively.

The % change in the latent heat (ΔH) was calculated using the following equation 8:

$$\%\ \text{change in } \Delta H = \frac{[\Delta H_{\text{Treated}} - \Delta H_{\text{Control}}]}{\Delta H_{\text{Control}}} \times 100 \quad (8)$$

Where $\Delta H_{Control}$ and $\Delta H_{Treated}$ are the latent heat of the control and treated berberine chloride, respectively.

## Results and Discussion

### Powder X-ray Diffraction (PXRD) Analysis

The PXRD diffractograms containing the Bragg's angle and intensity of the characteristic peaks of the control and the Biofield Energy Treated berberine chloride samples are shown in Figure 1. The further analysis of the diffractograms regarding the differences in the peak intensities and crystallite sizes of both the samples were mentioned in Table 1.

| Entry No. | Bragg angle (°2θ) | | Intensity (cps) | | | Crystallite size (G, nm) | | |
|---|---|---|---|---|---|---|---|---|
| | Control | Treated | Control | Treated | % change* | Control | Treated | % change* |
| 1 | 8.93 | 9.12 | 337 | 240 | -28.78 | 114 | 315 | 176.32 |
| 2 | 13.87 | 13.96 | 66 | 142 | 115.15 | 165 | 139 | -15.76 |
| 3 | 14.56 | 14.61 | 84 | 115 | 36.9 | 252 | 351 | 39.29 |
| 4 | 16.17 | 16.3 | 126 | 159 | 26.19 | 216 | 215 | -0.46 |
| 5 | 20.2 | 20.36 | 86 | 103 | 19.77 | 257 | 275 | 7 |
| 6 | 20.81 | 20.96 | 74 | 90 | 21.62 | 305 | 269 | -11.8 |
| 7 | 24.48 | 24.61 | 349 | 429 | 22.92 | 141 | 163 | 15.6 |
| 8 | 25.3 | 25.53 | 598 | 621 | 3.85 | 187 | 224 | 19.79 |
| 9 | 26.7 | 26.09 | 455 | 528 | 16.04 | 29 | 99 | 241.38 |

*denotes the percentage change in the peak intensity and crystallite size of the Biofield Energy Treated sample with respect to the control sample

Table 1: PXRD data for the control and Biofield Energy Treated berberine chloride.

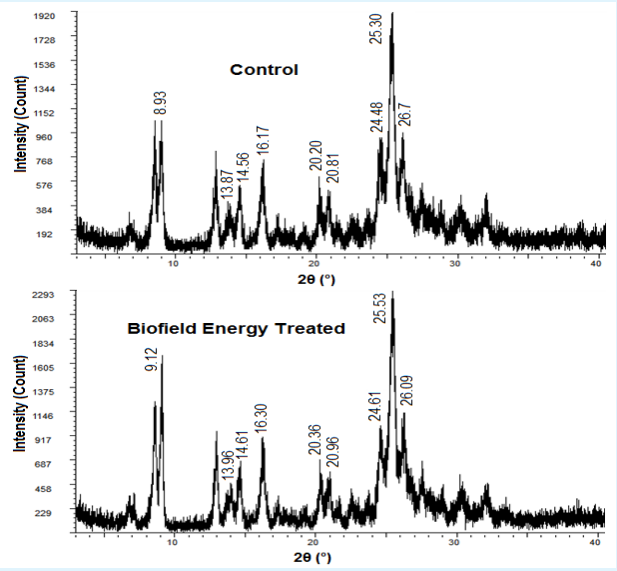


Figure 1: PXRD diffractograms of the control and Biofield Energy Treated berberine chloride.

The data indicated some major changes in the Bragg's angles of the treated sample as compared to the control sample. Moreover, the intensities of the characteristic peaks of the treated sample and the corresponding crystallite sizes also showed major alterations in comparison to the control sample. The peak intensities and crystallite sizes of the treated berberine chloride sample were observed to be significantly altered ranging from -28.78% to 115.15% and-15.76% to 241.38%, respectively, compared to the control sample. The average crystallite size of the Biofield Energy Treated sample was found as 227.78 nm, which was significantly increased by 23.05% compared the control sample (185.11 nm). The Biofield Energy Treatment has been known nowadays for its ability to alter the crystalline properties of the compounds by changing the Bragg's angle of the characteristic peaks of the diffractograms and their corresponding peak intensities and crystallite size, which indicated the formation of a novel polymorph [47]. Hence, it is presumed that there might be the formation of a novel polymorphic form of berberine chloride with some altered characteristics in comparison to the untreated sample. Besides, such alterations in crystal habit may be useful in improving the solubility and dissolution of the compound that ultimately affects its bioavailability profile [48].

## Particle Size Analysis (PSA)

The particle size analysis corresponding to $d_{10}$, $d_{50}$, $d_{90}$, and D (4,3) for both the samples was done and results are mentioned in Table 2. The analysis indicated that the treated berberine chloride sample showed significant changes in its particle size distribution as the particle sizes at $d_{10}$, $d_{50}$, $d_{90}$, and D (4,3) were significantly reduced by 16.89%, 34.41%, 21.88%, and 22.85%, respectively, in comparison to the control sample.

Therefore, the treated sample showed a considerable increase in its specific surface area by 14.74% that might occur due to the reduced particle size after the Biofield Energy Treatment of berberine chloride compared to the control sample. Various researchers studied the direct relationship between the particle size distribution of any drug and its performance in terms of dissolution, solubility, absorption, and bioavailability [49,50]. In addition, reducing the particle size and thereby increasing the surface area is used by various scientists in improving the bioavailability of compound [51]. Thus, it could be concluded that the treated berberine chloride might show better bioavailability after the Biofield Energy Treatment as compared to the control sample.

| Parameter | $d_{10}$ (µm) | $d_{50}$ (µm) | $d_{90}$ (µm) | D(4,3)(µm) | SSA($m^2$/g) |
|---|---|---|---|---|---|
| Control | 3.02 | 21.04 | 164.43 | 57.5 | 0.95 |
| Biofield Energy Treated | 2.51 | 13.8 | 128.45 | 44.36 | 1.09 |
| Percent change* (%) | -16.89 | -34.41 | -21.88 | -22.85 | 14.74 |

Table 2: Particle size distribution of the control and Biofield Energy Treated berberine chloride.

$d_{10}$, $d_{50}$, and $d_{90}$: particle diameter corresponding to 10%, 50%, and 90% of the cumulative distribution, D(4,3): the average mass-volume diameter, and SSA: the specific surface area. *denotes the percentage change in the particle size distribution of the Biofield Energy Treated sample with respect to the control sample.

## Thermal Gravimetric Analysis (TGA)/ Differential Thermogravimetric Analysis (DTG)

The TGA/DTG study helps in analysing the thermal degradation pattern of the control and treated sample on heating; and the data regarding weight loss, residue, and maximum degradation temperature (Tmax) was reported in Table 3. The scientific literature reported the thermal stability of berberine chloride up to 350 K after which the TGA curve showed four-step weight loss in the temperature range of 350 K to 520 K [52]. The analysis of TGA thermograms (Figure 2) of the control and the treated samples reported similar data as mentioned in the literature. Besides, the TGA analysis revealed that the weight loss during thermal degradation of the treated sample was slightly increased by 3.98%, which caused 3.64% reduction in the residue weight as compared to the control sample (Table 3).

| Sample | TGA | | DTG | | | |
|---|---|---|---|---|---|---|
| | | | $T_{max}$ (°C) | | | |
| | Total weight loss (%) | Residue % | Peak 1 | Peak 2 | Peak 3 | Peak 4 |
| Control | 47.77 | 52.23 | 78.28 | 182.37 | 298.35 | 386.1 |
| Biofield Energy Treated | 49.67 | 50.33 | 83.79 | 185.52 | 302.46 | 397.56 |
| % Change* | 3.98 | -3.64 | 7.04 | 1.73 | 1.38 | 2.97 |

*denotes the percentage change of the Biofield Energy Treated sample with respect to the control sample, $T_{max}$ = the temperature at which maximum weight loss takes place in TG or peak temperature in DTG.

Table 3: TGA/DTG data of the control and Biofield Energy treated samples of berberine chloride.

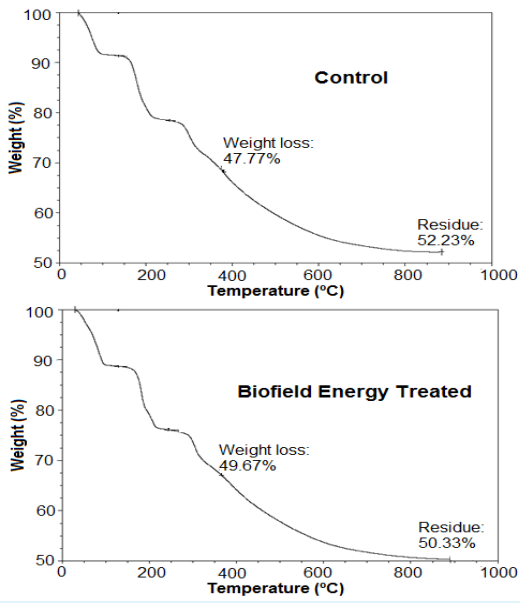


Figure 2: TGA thermograms of the control and Biofield Energy Treated berberine chloride.

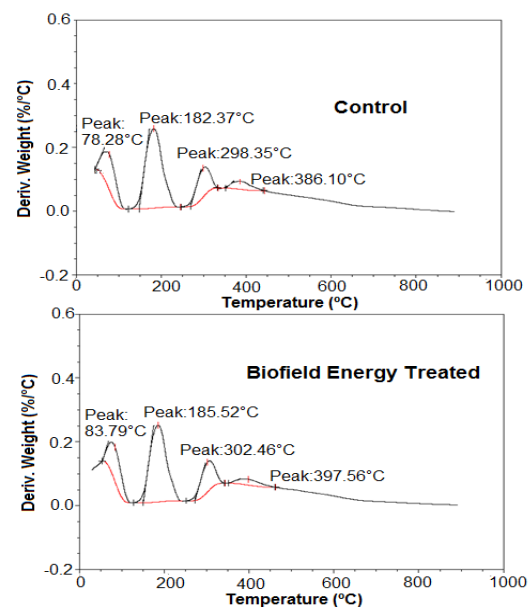


Figure 3: DTG thermograms of the control and Biofield Energy Treated berberine chloride.

Besides, the literature also reported the presence of four peaks in the DTG curve of berberine chloride that represented the various thermal decomposition products as $H_2O$ (379K), CO (421K), CO (490K), and $H_2O$ (514K) [52]. The DTG thermograms of the control and treated samples also revealed four peaks (Figure 3) with similar temperature as reported earlier. The comparative study of both samples indicated that the maximum thermal degradation temperature ($T_{max}$) corresponding to the 1st, 2nd, 3rd, and 4th Peak of the treated berberine chloride was increased by 7.04%, 1.73%, 1.38% and 2.97%, respectively compared to the control sample. Thus, the thermal analysis showed that the degradation temperature was increased in the treated sample after the Biofield Energy Treatment; thereby, indicating the improved thermal stability of the Biofield Energy Treated sample compared to the untreated sample.

## Differential Scanning Calorimetry (DSC) Analysis

The DSC analysis helps in studying the melting and degradation pattern of berberine chloride [53]. The analysis of thermograms of both the samples revealed the presence of six peaks in their thermograms (Figure 4). It was observed that the peak temperatures corresponding to 1st, 2nd, 3rd, and 4th Peak of the Biofield Energy Treated sample were significantly increased by 11.03%, 1.19%, 14.96%, and 2.18%, respectively; however, it was slightly reduced by 2.03% and 0.10% for the 5th and 6th Peak, respectively compared to the control samples. The treated sample also showed significant alterations in the latent heat of fusion (ΔH) corresponding to each peak as the ΔH corresponding to 1st, 2nd, 3rd, 4th, 5th, and 6th peak were significantly altered by 224.78%, 7.93%, 8.92%, -9.05%, -45.82%, and 10.93%, respectively, in comparison to the control sample (Table 4).

| Peak | Description | Peak Temperature (°C) | ΔH(J/g) |
|---|---|---|---|
| Peak 1 | Control sample | 87.66 | 6.98 |
| | Biofield Treated sample | 97.33 | 22.67 |
| | % Change* | 11.03 | 224.78 |
| Peak 2 | Control sample | 150.89 | 157.6 |
| | Biofield Treated sample | 152.68 | 170.1 |
| | % Change* | 1.19 | 7.93 |
| Peak 3 | Control sample | 178.78 | 83.17 |
| | Biofield Treated sample | 205.53 | 90.59 |
| | % Change* | 14.96 | 8.92 |
| Peak 4 | Control sample | 217.3 | 46.65 |
| | Biofield Treated sample | 222.04 | 42.43 |
| | % Change* | 2.18 | -9.05 |
| Peak 5 | Control sample | 291.31 | 51.51 |
| | Biofield Treated sample | 285.4 | 27.91 |
| | % Change* | -2.03 | -45.82 |
| Peak 6 | Control sample | 315.81 | 169.2 |
| | Biofield Treated sample | 315.48 | 187.7 |
| | % Change* | -0.1 | 10.93 |

ΔH: Latent heat of fusion; *denotes the percentage change of the Biofield Energy treated sample with respect to the control sample.

Table 4: Comparison of DSC data between the control and Biofield Energy treated berberine chloride.

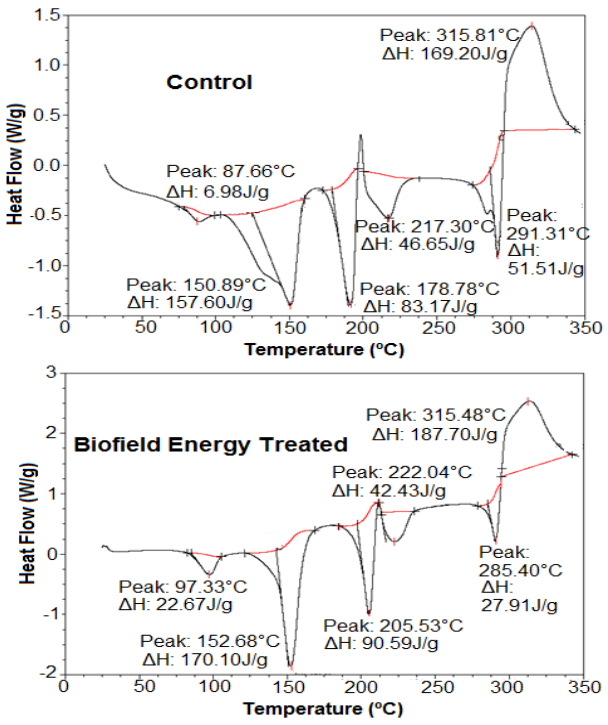


Figure 4: DSC thermograms of the control and Biofield Energy treated berberine chloride.

The study indicated major changes in the melting temperature and ΔH of the 1st peak of the treated sample that was increased significantly compared with the control sample. The other data also showed the improved thermal stability of treated berberine chloride sample along with the altered latent heat that might take place because of some significant changes in the crystallization structure of the Biofield Energy Treated sample [53].

## Conclusions

The Trivedi Effect®-Consciousness Energy Healing Treatment has shown a significant impact on the physicochemical properties of berberine chloride in comparison to the control sample. The PXRD peak intensities and crystallite sizes altered ranging from-28.78% to 115.15% and -15.76% to 241.38%, respectively, in comparison to the control sample. Besides, the average crystallite size of the treated sample was significantly increased by 23.05% compared to the untreated berberine chloride sample. It is suggested that such changes have taken place as the Biofield Energy Treatment might create some new polymorph of berberine chloride that could be evident from the major changes in the crystalline properties of the treated sample. The particle size data showed significant variations in the size distribution of the berberine sample after the Biofield Energy Treatment as the particle sizes were significantly reduced by 16.89%, 34.41%, 21.88%, and 22.85%, at d10, d50, d90, and D(4,3), respectively in comparison to the control sample. The changes in the particle sizes affected thespecific surface area of the treated sample, which was observed to be increased by 14.74% compared to the control sample. Such changes might attribute the significant alterations in the bioavailability profile of the treated sample by enhancing the solubility, dissolution, and absorption parameters. The TGA study revealed the increase i.e., 3.98%, in the total weight loss of the treated sample and 3.64% decrease in the residue weight of the treated berberine chloride compared to the untreated sample. However, the Tmax corresponding to the 1st, 2nd, 3rd, and 4th peak of the treated sample was increased by 7.04%, 1.73%, 1.38%, and 2.97%, respectively compared to the untreated berberine chloride sample. The DSC data revealed that the melting point of 1st, 2nd, 3rd, and 4th peak of the treated berberine chloride sample were increased by 11.03%, 1.19%, 14.96%, and 2.18%, respectively, compared to the control sample. The latent heat for the 1st, 2nd, 3rd, 4th, 5th, and 6th peaks of the treated sample were significantly altered by 224.78%, 7.93%, 8.92%, -9.05%, -45.82%, and 10.93%, respectively, compared to the control sample.The results indicated that the Biofield Energy Treatment might improve the degradation temperature of the treated sample that ultimately helps in improving its thermal stability as compared to the control sample. Thus, it was concluded that the Trivedi Effect®-Consciousness Energy Healing Treatment significantly affect the crystalline properties, particle sizes, surface area, and thermal stability of the berberine chloride sample. The Biofield Energy Treatment might form a new polymorph that may show better solubility, absorption,thermal stability, and bioavailability in comparison to the untreated sample. Hence, the Biofield EnergyTreated sample could be used in the form ofnovel drug and might be used to formulate new pharmaceutical/nutraceutical products that would be more effective in the treatment of various diseases such as glaucoma, ailments related to eye and skin, diarrhea, gastric ulcers, tumor, polycystic ovary syndrome, gastroenteritis, menopausal symptoms, hypertension, high cholesterol, inflammation, malaria, hyperglycemia, congestive heart failure, arrhythmia, metabolic syndromes, thrombocytopenia, obesity, osteoporosis, liver diseases, trachoma, etc.

## Acknowledgements

The authors are grateful to Central Leather Research Institute, SIPRA Lab. Ltd., Trivedi Science, Trivedi Global,

Inc., Trivedi Testimonials, and Trivedi Master Wellness for their assistance and support during this work.

## References

1. Yin J, Zhang H, Ye J (2008) Traditional chinese medicine in treatment of metabolic syndrome. EndocrMetab Immune Disord Drug Targets 8(2): 99-111.

2. Mohammadzadeh N, Mehri S, Hosseinzadeh H (2017) *Berberis vulgaris* and its constituent berberine as antidotes and protective agents against natural or chemical toxicities. Iran J Basic Med Sci 20(5): 538-551.

3. Zuo F, Nakamura N, Akao T, Hattori M (2006) Pharmacokinetics of berberine and its main metabolites in conventional and pseudo germ-free rats determined by liquid chromatography/ion trap mass spectrometry. Drug Metab Dispos 34(12): 2064-2072.

4. Dutta D, Kalra S, Sharma M (2017) Adenosine monophosphate-activated protein kinase-based classification of diabetes pharmacotherapy. J Postgrad Med 63(2): 114-121.

5. Lee YS, Kim WS, Kim KH, Yoon MJ, Cho HJ, et al. (2006) Berberine, a natural plant product, activates AMP-activated protein kinase with beneficial metabolic effects in diabetic and insulin-resistant states. Diabetes 55(8): 2256-2264.

6. Srivastava RA, Pinkosky SL, Filippov S, Hanselman JC, Cramer CT, et al. (2012) AMP-activated protein kinase: an emerging drug target to regulate imbalances in lipid and carbohydrate metabolism to treat cardio-metabolic diseases. J Lipid Res 53: 2490-2514.

7. DeFilipps RA, Krupnick GA (2018) The medicinal plants of Myanmar. Phyto Keys 102: 1-341.

8. Wei W, Zhao H, Wang A, Sui M, Liang K, et al. (2012) A clinical study on the short-term effect of berberine in comparison to metformin on the metabolic characteristics of women with polycystic ovary syndrome. Eur J Endocrinol 166(1): 99-105.

9. Birdsall T, Kelly G (1997) Berberine: therapeutic potential of an alkaloid found in several medicinal plants. Alt Med Rev2(2): 94-103.

10. Schor J (2012) Clinical Applications for Berberine: Potential therapeutic applications in metabolic syndrome, type 2 diabetes, and dyslipidemia. Natural Medicine Journal 4.

11. Zhang H, Wei J, Xue R, Wu JD, Zhao W, et al. (2010) Berberine lowers blood glucose in type 2 diabetes mellitus patients through increasing insulin receptor expression. Metabolism59(2): 285-292.

12. Kong W, Wei J, Abidi P, Lin M, Inaba S, et al. (2004) Berberine is a novel cholesterol-lowering drug working through a unique mechanism distinct from statins. Nat Med 10(12): 1344-1351.

13. Tsai PL, Tsai TH (2004) Hepatobiliary excretion of berberine. Drug Metab Dispos 32(4): 405-412.

14. Ye M, Fu S, Pi R, He F (2009) Neuropharmacological and pharmacokinetic properties of berberine: a review of recent research. J Pharm Pharmacol 61(7): 831-837.

15. Khadka P, Ro J, Kim H, Kim I, Kim JT, et al. (2014) Pharmaceutical particle technologies: An approach to improve drug solubility, dissolution and bioavailability. Asian J Pharm 9(6): 304-316.

16. Movaffaghi Z, Farsi M (2009) Biofield therapies: Biophysical basis and biological regulations. Complement Ther Clin Pract 15(1): 35-37.

17. Barnes PM, Powell-Griner E, McFann K, Nahin RL (2004) Complementary and alternative medicine use among adults: United States, 2002. Adv Data 343: 1-19.

18. Barnes PM, Bloom B, Nahin RL (2008) Complementary and alternative medicine use among adults and children: United States, 2007. Natl Health Stat Report 12: 1-23.

19. Wai FK (2005) National Center for Complementary and Alternative Medicine Website. J Med LibrAssoc 93: 410-412.

20. Trivedi MK, Tallapragada RM (2008) A transcendental to changing metal powder characteristics. Met Powder Rep 63(9): 22-28, 31.

21. Trivedi MK, Nayak G, Patil S, Tallapragada RM, Latiyal O (2015) Studies of the atomic and crystalline characteristics of ceramic oxide nano powders after bio field treatment. Ind Eng Manage 4: 161.

22. Trivedi MK, Nayak G, Patil S, Tallapragada RM, Latiyal O, et al. (2015) Effect of biofield energy treatment on physical and structural properties of calcium carbide and praseodymium oxide. International Journal of Materials Science and Applications 4(6): 390-395.

23. Trivedi MK, Branton A, Trivedi D, Nayak G, Mondal SC, et al. (2015) Morphological characterization, quality, yield and DNA fingerprinting of biofield energy treated alphonso mango (*Mangiferaindica* L.). Journal of Food and Nutrition Sciences 3(6): 245-250.

24. Trivedi MK, Branton A, Trivedi D, Nayak G, Mondal SC, et al. (2015) Evaluation of biochemical marker – Glutathione and DNA fingerprinting of biofield energy treated *Oryza sativa*. American Journal of BioScience 3(6): 243-248.

25. Trivedi MK, Branton A, Trivedi D, Nayak G, Charan S, et al. (2015) Phenotyping and 16S rDNA analysis after biofield treatment on *Citrobacter braakii*: A urinary pathogen. J Clin Med Genom 3: 129.

26. Trivedi MK, Patil S, Shettigar H, Mondal SC, Jana S (2015) Evaluation of biofield modality on viral load of Hepatitis B and C viruses. J Antivir Antiretrovir 7: 083-088.

27. Trivedi MK, Patil S, Shettigar H, Mondal SC, Jana S (2015) An impact of biofield treatment: Antimycobacterial susceptibility potential using BACTEC 460/MGIT-TB System. Mycobact Dis 5: 189.

28. Trivedi MK, Patil S, Shettigar H, Bairwa K, Jana S (2015) Phenotypic and biotypic characterization of *Klebsiella oxytoca*: An impact of biofield treatment. J Microb Biochem Technol 7: 203-206.

29. Nayak G, Altekar N (2015) Effect of biofield treatment on plant growth and adaptation. J Environ Health Sci 1(2): 1-9.

30. Branton A, Jana S (2017) The influence of energy of consciousness healing treatment on low bioavailable resveratrol in male *Sprague Dawley* rats. International Journal of Clinical and Developmental Anatomy 3(3): 9-15.

31. Branton A, Jana S (2017) The use of novel and unique biofield energy healing treatment for the improvement of poorly bioavailable compound, berberine in male Sprague Dawley rats. American Journal of Clinical and Experimental Medicine 5(4): 138-144.

32. Branton A, Jana S (2017) Effect of The biofield energy healing treatment on the pharmacokinetics of 25-hydroxyvitamin $D_3$ [25(OH)$D_3$] in rats after a single oral dose of vitamin $D_3$. American Journal of Pharmacology and Phytotherapy 2(1): 11-18.

33. Kinney JP, Trivedi MK, Branton A, Trivedi D, Nayak G, et al. (2017) Overall skin health potential of the biofield energy healing based herbomineral formulation using various skin parameters. American Journal of Life Sciences 5(2): 65-74.

34. Singh J, Trivedi MK, Branton A, Trivedi D, Nayak G, et al. (2017) Consciousness energy healing treatment based herbomineral formulation: A safe and effective approach for skin health. American Journal of Pharmacology and Phytotherapy 2(1): 1-10.

35. Trivedi MK, Branton A, Trivedi D, Nayak G, Plikerd WD, et al. (2017) A Systematic study of the biofield energy healing treatment on physicochemical, thermal, structural, and behavioral properties of magnesium gluconate. International Journal of Bioorganic Chemistry 2(3): 135-145.

36. Trivedi MK, Branton A, Trivedi D, Nayak G, Plikerd WD, et al. (2017) Chromatographic and spectroscopic characterization of the consciousness energy healing treated *Withania Somnifera* (ashwagandha) root extract. European Journal of Biophysics 5(2): 38-47.

37. Trivedi MK, Patil S, Shettigar H, Mondal SC, Jana S (2015) The potential impact of biofield treatment on human brain tumor cells: A time-lapse video microscopy. J Integr Oncol 4(3): 141.

38. Trivedi MK, Patil S, Shettigar H, Gangwar M, Jana S (2015) *In vitro* evaluation of biofield treatment on cancer biomarkers involved in endometrial and prostate cancer cell lines. J Cancer Sci Ther 7: 253-257.

39. Anagnos D, Trivedi K, Branton A, Trivedi D, Nayak G, et al. (2018) Influence of biofield treated vitamin $D_3$ on proliferation, differentiation, and maturation of bone-related parameters in MG-63 cell-line. International Journal of Biomedical Engineering and Clinical Science 4: 6-14.

40. Lee AC, Trivedi K, Branton A, Trivedi D, Nayak G, et al. (2018) The potential benefits of biofield energy treated vitamin D3 on bone mineralization in human bone osteosarcoma cells (MG-63). International Journal of Nutrition and Food Sciences 7: 30-38.

41. Stutheit ME, Trivedi K, Branton A, Trivedi D, Nayak G, et al. (2018) Biofield energy treated vitamin $D_3$: Therapeutic implication on bone health using osteoblasts cells. American Journal of Life Sciences 6: 13-21.

42. Desktop X-ray Diffractometer "MiniFlex+"(1997) The Rigaku Journal 14: 29-36.

43. Zhang T, Paluch K, Scalabrino G, Frankish N, Healy AM, Sheridan H (2015) Molecular structure studies of (1S,2S)-2-benzyl-2,3-dihydro-2-(1Hinden-2-yl)-1H-inden-1-ol. J Mol Struct 1083: 286-299.

44. Langford JI, Wilson AJC (1978) Scherrer after sixty years: A survey and some new results in the determination of crystallite size. J ApplCryst 11(2): 102-113.

45. Trivedi MK, Sethi KK, Panda P, Jana S (2017) Physicochemical, thermal and spectroscopic characterization of sodium selenate using XRD, PSD, DSC, TGA/DTG, UV-vis, and FT-IR. Marmara Pharmaceutical Journal 21(2): 311-318.

46. Trivedi D, Trivedi MK, Branton A, Trivedi D (2018) Impact of Consciousness Energy Healing Treatment on the Physicochemical and Thermal Properties of Vitamin $D_3$ (Cholecalciferol). Food Sci Nutr Technol 3: 000162.

47. Trivedi MK, Branton A, Trivedi D, Nayak G, Lee AC, et al. (2017) Evaluation of the impact of biofield energy healing treatment (the Trivedi Effect®) on the physicochemical, thermal, structural, and behavioural properties of magnesium gluconate. International Journal of Nutrition and Food Sciences 6(2): 71-82.

48. Savjani KT, Gajjar AK, Savjani JK (2012) Drug Solubility: Importance and Enhancement Techniques. ISRN Pharmaceutics 2012: 10.

49. Loh ZH, Samanta AK, Heng PWS (2015) Overview of milling techniques for improving the solubility of poorly water-soluble drugs. Asian J Pharm 10(4): 255-274.

50. Khadkaa P, Roa J, Kim H, Kim I, Kim JT, et al. (2014) Pharmaceutical particle technologies: An approach to improve drug solubility, dissolution and bioavailability. Asian J Pharm 9: 304-316.

51. Hu J, Johnston KP, Williams RO (2004) Nanoparticle engineering processes for enhancing the dissolution rates of poorly water soluble drugs. Drug Dev Ind Pharm 30(3): 233-245.

52. Cheng XX, Lui Y, Hu YJ, Liu Y, Li LW, et al. (2009) Thermal behavior and thermodynamic properties of berberine hydrochloride. J Therm Anal Calorim.

53. Zhao Z, Xie M, Li Y, Chen A, Li G, et al. (2015) Formation of curcumin nanoparticles *via* solution enhanced dispersion by supercritical $CO_2$. Int J Nanomedicine 10: 3171-3181.